Available online at www.sciencedirect.com
SCIENCE DIRECT®
Icarus 182 (2006) 406–412
ICARUS
www.elsevier.com/locate/icarus

Plasma intrusion above Mars crustal fields—Mars Express ASPERA-3 observations

M. Fränz [a,*], J.D. Winningham [b], E. Dubinin [a], E. Roussos [a], J. Woch [a], S. Barabash [c], R. Lundin [c], M. Holmström [c], H. Andersson [c], M. Yamauchi [c], A. Grigoriev [c], R.A. Frahm [b], J.R. Sharber [b], J.R. Scherrer [b], A.J. Coates [d], Y. Soobiah [d], D.R. Linder [d], D.O. Kataria [d], E. Kallio [e], T. Säles [e], P. Riihelä [e], W. Schmidt [e], H.E.J. Koskinen [f], J. Kozyra [g], J. Luhmann [h], E. Roelof [i], D. Williams [i], S. Livi [i], C.C. Curtis [j], K.C. Hsieh [j], B.R. Sandel [j], M. Grande [k], M. Carter [k], J.-A. Sauvaud [l], A. Fedorov [l], J.-J. Thocaven [l], S. McKenna-Lawler [m], S. Orsini [n], R. Cerulli-Irelli [n], M. Maggi [n], P. Wurz [o], P. Bochsler [o], N. Krupp [a], K. Asamura [p], C. Dierker [q]

[a] *MPI für Sonnensystemforschung, Max-Planck-Str. 2, 37191 Katlenburg-Lindau, Germany*
[b] *Southwest Research Institute, San Antonio, TX 7228-0510, USA*
[c] *Swedish Institute of Space Physics, Box 812, S-98 128, Kiruna, Sweden*
[d] *Mullard Space Science Laboratory, University College London, Surrey RH5 6NT, UK*
[e] *Finnish Meteorological Institute, Box 503, FIN-00101 Helsinki, Finland*
[f] *Department of Physical Sciences, University of Helsinki, P.O. Box 64, 00014 Helsinki, Finland*
[g] *Space Physics Research Laboratory, University of Michigan, Ann Arbor, MI 48109-2143, USA*
[h] *Space Science Laboratory, University of California in Berkeley, Berkeley, CA 94720-7450, USA*
[i] *Applied Physics Laboratory, Johns Hopkins University, Laurel, MD 20723-6099, USA*
[j] *University of Arizona, Tucson, AZ 85721, USA*
[k] *Rutherford Appleton Laboratory, Chilton, Didcot, Oxfordshire OX11 0QX, UK*
[l] *Centre d'Etude Spatiale des Rayonnements, BP-4346, F-31028 Toulouse, France*
[m] *Space Technology Ireland, National University of Ireland, Maynooth, Co. Kildare, Ireland*
[n] *Istituto di Fisica dello Spazio Interplanetari, I-00133 Rome, Italy*
[o] *Physikalisches Institut, University of Bern, CH-3012 Bern, Switzerland*
[p] *Institute of Space and Astronautical Science, 3-1-1 Yoshinodai, Sagamichara, Japan*
[q] *Technical University of Braunschweig, Hans-Sommer-Strasse 66, D-38106 Braunschweig, Germany*

Received 21 March 2005; revised 16 August 2005

Available online 27 January 2006

Abstract

Using data of the ASPERA-3 instrument on board the European Mars Express spacecraft we investigate the effect of the martian crustal fields on electrons intruding from the magnetosheath. For the crustal field strength we use published data obtained by the Mars Global Surveyor MAG/ER instrument for a fixed altitude of 400 km. We use statistics on 13 months of 80–100 eV electron observations to show that the electron intrusion altitude determined by a probability measure is approximately linearly dependent on the total field strength at 400 km altitude. We show that on the dayside the mean electron intrusion altitude describes the location of the Magnetic Pile-Up Boundary (MPB) such that we can quantify the effect of the crustal fields on the MPB. On the nightside we quantify the shielding of precipitating electrons by the crustal fields.

PACS: 96.30.Gc; 94.05.-a; 96.12.Jt

* Corresponding author.
E-mail address: fraenz@mps.mpg.de (M. Fränz).

0019-1035/$ – see front matter
doi:10.1016/j.icarus.2005.11.016

Keywords: Mars; Magnetospheres

1. Introduction

Since the discovery of the martian crustal magnetization (Acuña et al., 1998) there have been numerous studies to investigate the effects of the crustal fields on the plasma environment of Mars (see Connerney et al. (2004) and Brain (2003) for reviews and Lillis et al. (2004) and Crider (2004) for recent studies). The observations used in all these studies have been using data from the Mars Global Surveyor (MGS) magnetometer and electron reflectometer instrument MAG/ER (Acuña et al., 2001). The combination of magnetic field and electron data from MGS allowed to separate open and closed field lines and map the influence on the field line topology as a function of solar zenith angle and interplanetary field orientation in great detail (Brain et al., 2003). Fig. 1 shows a sketch of the location of the martian crustal fields in the southern martian hemisphere together with the main plasma boundaries in the martian solar orbital (MSO) xz-plane. The Sun is towards the positive x-axis, and the z-axis is perpendicular to the Mars orbital plane (positive northward). In this paper we call the inner boundary of the magnetosheath magnetic pile-up boundary (MPB) since it is more common than the term induced magnetospheric boundary (IMB), which is sometimes taken when particle observations are used for the identification. Whether there is any difference between the boundary determined by particle observations and field observations has not been proven.

Using magnetometer observations only it could be qualitatively shown that the crustal fields move the MPB outward (Crider et al., 2002). As well Vignes et al. (2002) have shown that the bow shock altitude is independent of local crustal fields. While all these studies have improved our knowledge about the distances at which martian crustal fields can have an influence on the plasma environment, it has not been studied how the fields affect the plasma intrusion from the magnetosheath into the atmosphere. Also it has so far not been attempted to quantify the relation between crustal field strength and MPB altitude. In this paper we address both questions.

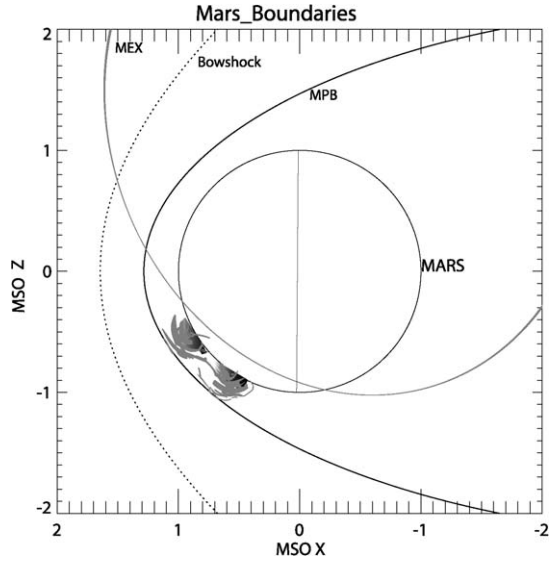

Fig. 1. Sketch showing the location of the bowshock and magnetic pile-up boundary (MPB, also called induced magnetospheric boundary IMB) as determined by Vignes et al. (2000) together with the Orbit of Mars Express (MEX) in May 2004 in a MSO xz coordinate plane. The $+x$-axis points toward the Sun, the z-axis is perpendicular to the Mars orbit. In the southern hemisphere of Mars the location of crustal fields is suggested.

Another effect of the crustal field is the focusing of electron precipitation in local cusps. This can lead to auroral effects as they recently have been observed by the Mars Express ultraviolet spectrometer (Bertaux et al., 2005). These local structures are discussed in more detail in an accompanying paper in this issue (Soobiah et al., 2006). In this paper we only discuss the statistical effect of these events.

Here we report on observations by the ASPERA-3 plasma analyzer on board the Mars Express spacecraft (MEX) (Barabash et al., 2004). The ASPERA-3 instrument has separate sensors for neutral energetic atoms, protons, heavy ions and electrons. We use data of the electron sensor only to investigate how the intrusion depth of magnetosheath electrons depends on the local crustal field strength. Unfortunately the MEX spacecraft does not have a magnetometer on board that would allow us to determine electron pitch angles. But in comparison to the MGS observations MEX data have a better coverage of altitudes above 400 km.

2. Instrumentation and data

We use data of the ELS electron sensor of the ASPERA-3 instrument on board the Mars Express spacecraft (Barabash et al., 2004). The sensor is a top-hat electrostatic analyzer with an energy range of 0.4 eV–20 keV, an energy resolution of 8% and a field of view of $4° \times 360°$. The 360° aperture is divided into 16 sectors. In this paper we only use energy fluxes integrated over all 16 anodes and 80–100 eV energy. The energy flux is obtained by multiplying the count rate measured by the sensor by the geometric factor and the channel energy and dividing by the energy width of the channel. Units are $\mathrm{eV}/(\mathrm{cm}^2\,\mathrm{s}\,\mathrm{sr}\,\mathrm{eV})$. This energy range is above typical photo electron energies and characterizes the lower energy part of Martian magnetosheath electrons which have typical energies between 40 and 400 eV. Data are obtained at a time resolution of 4 s.

We use crustal field strength data interpolated on a regular grid for an altitude of 400 km from Mars Global Surveyor MAG/ER observations as presented by Connerney et al. (2001). The interpolation has a resolution of 1° in latitude and longitude and covers all latitudes between $-86°$ and $+86°$. Spatial coordinates are calculated using the SPICE system (http://naif.jpl.nasa.gov/naif/). Since the shielding is most efficient perpendicular to the vertically intruding electrons (Verigin et al., 2004) we used both the total value of the field and just the horizontal component. We observed that the total value is the

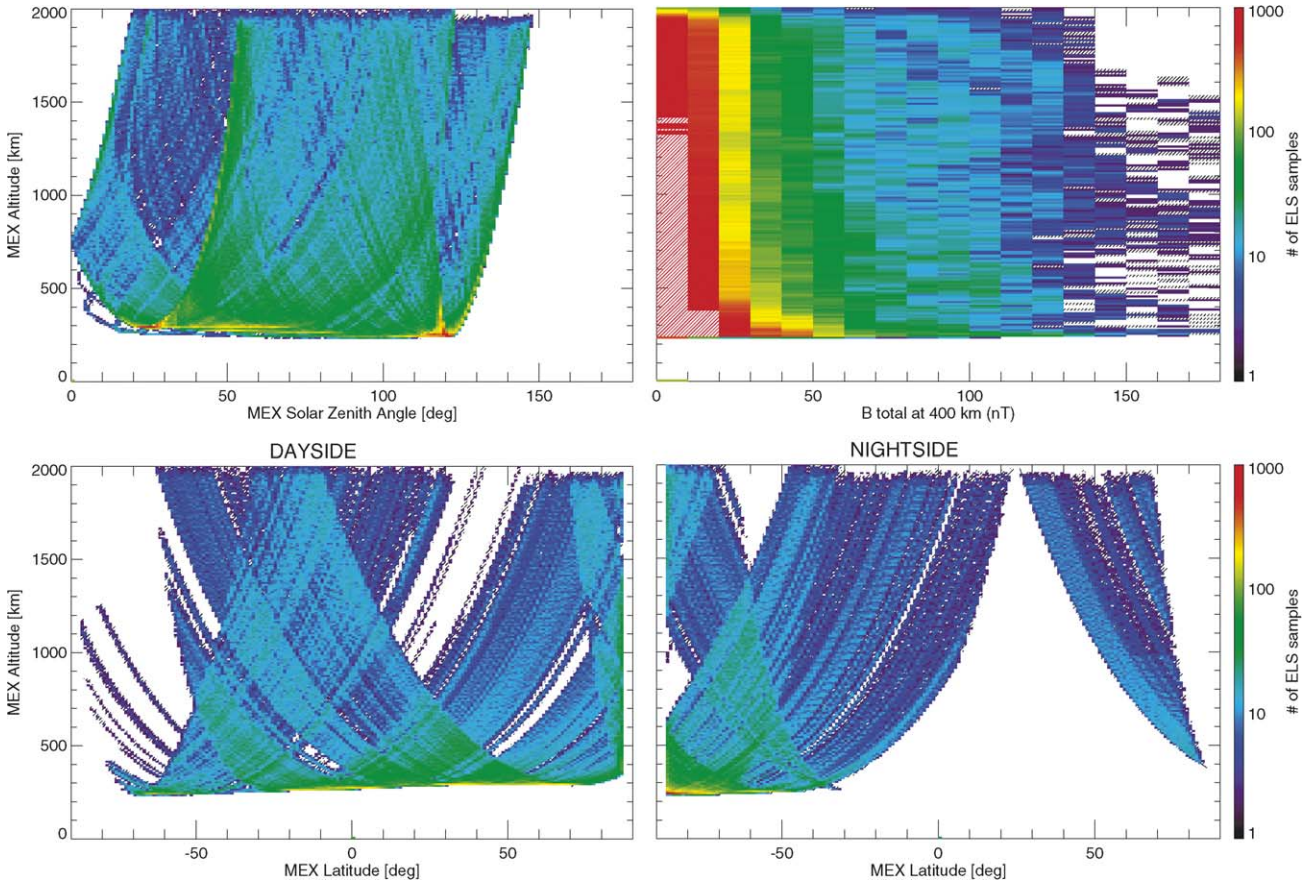

Fig. 2. Data coverage for the electron sensor data of the Mars Express ASPERA-3 instrument for all orbits between 1 Feb 2004 and 1 Mar 2005 as a function of (a) solar zenith angle and spacecraft altitude above surface, (b) MGS crustal field and spacecraft altitude above surface, (c) Mars planetocentric latitude and spacecraft altitude above surface for the dayside (SZA $< 90°$), (d) Mars planetocentric latitude and spacecraft altitude above surface for the nightside (SZA $> 90°$).

better proxy for the shielding effect when comparing data from a large altitude range.

Fig. 2 shows the data coverage for the electron sensor data of the Mars Express ASPERA-3 instrument for all orbits between 1 Feb 2004 and 1 Mar 2005 as a function of different orbital parameters below 2000 km altitude and of the crustal field strength below the MEX orbit. Bin sizes are 1° in angular coordinates and 10 km in altitude. Red shaded bins have values higher than the maximum of the color bar, black shaded bins have values lower or equal than the minimum of the color bar. Coverage is good for solar zenith angles between 15° and 120°. Martian latitudes below −50° on the dayside and above −20° on the nightside are poorly covered. The coverage is similar to the pre-mapping orbits of Mars Global Surveyor (Brain, 2003), but significantly better for solar zenith angles below 30° and on the nightside.

3. Local effects of crustal topology

Fig. 3 (top) shows the median energy flux of 80–100 eV electrons measured by the electron sensor of the Mars Express ASPERA-3 instrument below 800 km altitude on the nightside for all orbits between 1 Feb 2004 and 1 Mar 2005 as a function of Mars planetocentric eastern longitude and latitude for the southern hemisphere. The bottom panel shows the inverse of the total crustal field strength at 400 km altitude for the regions covered by the MEX orbit. We use the inverse of the field strength to have comparable color ranges in both panels. All data are binned at 2° resolution. On the nightside data coverage for the northern hemisphere is very poor and data are not shown here. The observations show that on large spatial scales electron fluxes are much lower above regions of high crustal field than in regions of low crustal field. But on scales of a few degrees we observe localized peaks in electron flux which may be associated with cusp-like structures above crustal field sources. Local crustal field observations by ASPERA-3 are also discussed in another paper in this issue (Soobiah et al., 2006). Statistics are not sufficient to map data limited to smaller altitude ranges in this way.

4. Plasma intrusion altitude

Fig. 4 shows the distribution of ELS data samples for three different regions of the magnetosphere: in the subsolar region of the magnetosheath (top panel), in a low field region for a medium altitude range on the dayside (middle) and on the nightside below the MPB (bottom) as a function of the logarithm of the energy flux in $\mathrm{eV}/(\mathrm{cm}^2\,\mathrm{s\,sr\,eV})$. In a non-logarithmic linear binning of the energy flux the centers of the distributions would be squashed to the left side. One can see that inside the

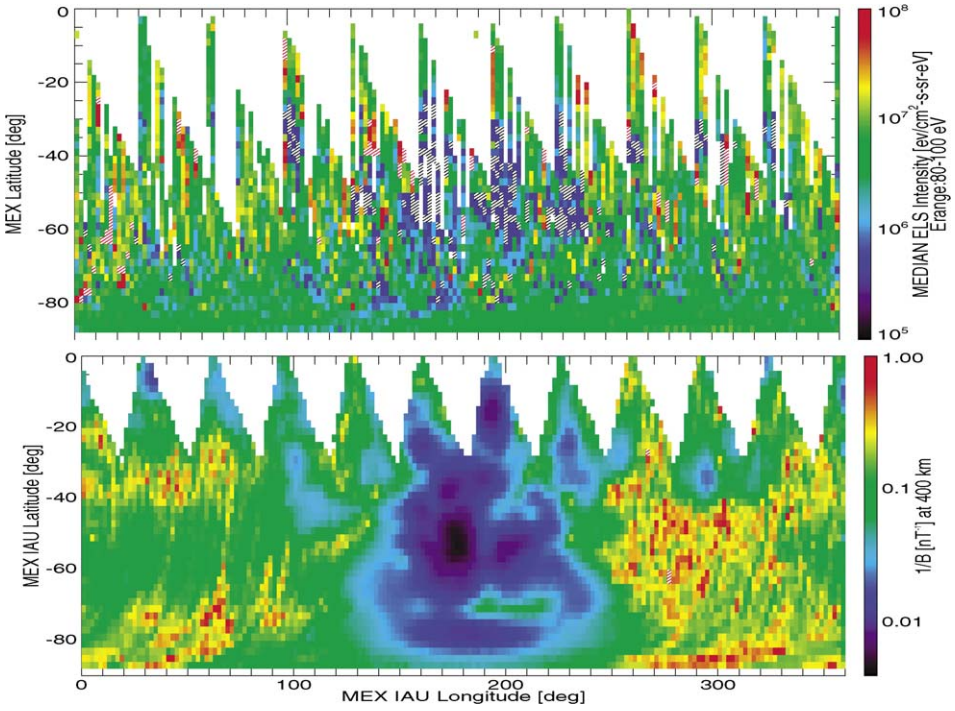

Fig. 3. (Top) Median energy flux of 80–100 eV electrons measured by the electron sensor of the Mars Express ASPERA-3 instrument below 800 km altitude on the nightside for all orbits between 1 Feb 2004 and 1 Mar 2005 as a function of Mars planetocentric eastern longitude and latitude. (Bottom) Inverse of the total crustal field strength (1/nT) at 400 km altitude from Connerney et al. (2001).

magnetosheath the distribution is Gaussian with a fitted mean of $10^{8.6}$ eV/(cm^2 s sr eV) and a small tail of low flux values. The small low-flux tail is caused by sampling solar wind above 1800 km altitude and is not the topic of this paper.

On the dayside the distribution can be separated into two distinct populations: One with a fitted median flux of about 10^7 eV/(cm^2 s sr eV), the other with a fitted median flux of about $10^{8.5}$ eV/(cm^2 s sr eV) (the median value divides the distribution such that the same number of samples is above and below (Press et al., 1992), for a purely Gaussian distribution it coincides with the center). We interpret this bimodality as the motion of the MPB: above the MPB the energy flux has a median value of $10^{8.6}$ eV/(cm^2 s sr eV), below a median value of 10^7 eV/(cm^2 s sr eV). An observer in a specific altitude/crustal field region is either located below the MPB or above depending on the solar wind and interplanetary field conditions at the time of observation. The log-normal distribution in the magnetosheath (top panel) shows that what we see at medium altitude range is not an oscillation between two states of the magnetosheath flux. If the change of energy flux across the MPB would happen on large spatial scales the distribution would not be bimodal but would show more samples of medium flux levels. This agrees with the observation that on a typical MEX orbit the transition happens in less than one minute. It also means that on average less than 2.5% of 100 eV electrons can penetrate the MPB. We will not extend on this topic here since the analysis of MPB crossings will be studied in a separate paper. Whether the 100 eV electrons observed below the MPB are of magnetosheath or ionospheric origin will also be studied separately.

The interpretation of two separate distributions is confirmed by the nightside distribution (Fig. 4, right): Here the MPB is on average located above 2000 km altitude (Fig. 1) such that even for times of strong solar wind pressure it is not observed below 800 km altitude. The high flux tail of the distribution on the nightside may be explained by intrusion events of aurora or polar rain type (Bertaux et al., 2005). For a bimodal distribution as observed on the dayside neither the median nor the mean are good estimators of the average of all data samples (Press et al., 1992). But if we take the middle point of the two Gaussians ($10^{7.8} = 6 \times 10^7$ eV/(cm^2 s sr eV)) as a separator we can determine for any region in the magnetosphere how often fluxes higher than the separation flux are observed. This method we will use in the following analysis.

The observations of diminished electron fluxes above areas of high magnetization led us to look at the latitudinal dependence of the fluxes as a function of crustal field strength. We took the digitized crustal field map at altitude 400 km by Connerney et al. (2001) to bin the ASPERA-3 electron observations as a function of local total crustal field below the orbital position of MEX.

Fig. 5 shows electron energy fluxes measured by the electron sensor of the Mars Express ASPERA-3 instrument for all orbits between 1 Feb 2004 and 1 Mar 2005 as a function of the total crustal field strength at 400 km altitude and MEX spacecraft altitude for altitudes below 1000 km. Bin sizes are 10 nT in field strength and 10 km in height. Red shaded bins have fluxes higher than or equal to the maximum value of the color bar, black shaded bins have fluxes lower than or equal to the minimum value of the color bar. Data coverage above 50 nT

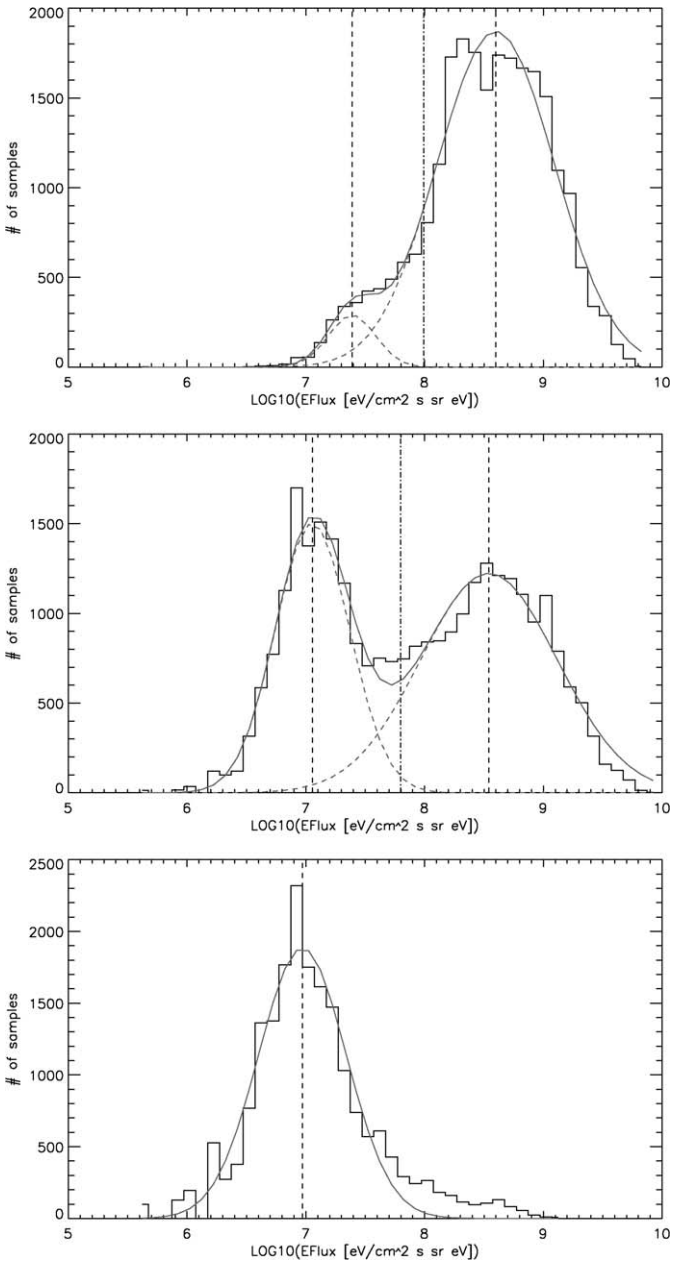

Fig. 4. Number of ELS 4s data samples collected between 1 Feb 2004 and 1 Mar 2005 in the sheath (between 1000 and 2000 km altitude and zenith angles below 45°, top); on the dayside (middle) and nightside (bottom) in the altitude range 600–800 km for crustal field regions below 20 nT. Data are binned as a function of the logarithm of the energy flux with a binsize of 0.1. The dashed vertical lines mark the Gaussian-fitted means, the dash-dotted lines the intersection point of the distributions.

is poor (see also Fig. 2). Panels on the left are for dayside observations, panels on the right for nightside observations (solar zenith angles smaller or larger than 90°). The top panels show the percentages of data samples above 6×10^7 eV/(cm^2 s sr eV) which we use as the flux value which divides electron populations above and below the MPB (see Fig. 4). The middle and bottom panels show median and maximum bin values, respectively.

Let us first consider the *dayside* observations. The percentages shown in Fig. 5 (top left) describe for the dayside how often at a specific altitude and above a certain field strength the spacecraft is inside the magnetosheath or in a local cusp. Thus it characterizes how low the MPB can be pressed against the additional force of the crustal fields. The average MPB location is determined by the 50% level. Above regions of low fields (<20 nT) the MPB is on average at 600 km altitude, while above high-field regions (>50 nT) it is observed at 800 km altitude. The dependence of the average MPB altitude on the field strength seems to be almost linear. The middle panels of Fig. 5 show the median fluxes. Because on the dayside the sample distribution is bimodal the median flux level is difficult to use quantitatively—except at the separator flux level (6×10^7 eV/(cm^2 s sr eV)) which marks the same bins as the 50% level in the percentage plot. But also the rest of the matrix qualitatively confirms the observation of the percentage plot. Notable are higher flux medians above higher fields in some altitude bins which can be interpreted as electron intrusion along cusps under certain solar wind conditions. The maximum bin values in Fig. 5 (bottom, left—note different scaling) show how deep the MPB can reach under extreme solar wind conditions on the dayside. The figure shows that even then the crustal fields shield efficiently up to 600 km altitude.

On the *nightside* (Fig. 5, right panels) MEX orbits until 1 March 2005 only cover solar zenith angles up to 130° (see Fig. 2), that is our observations are made close to the terminator and do not cover plumes closer to the center of the magnetotail. The percentages (top right) are below 20% almost everywhere and describe the high flux tail of the penetrating electron distribution. Since on the nightside we never cross the MPB we interpret the median and maximum fluxes (middle and bottom right) as the intrusion behavior similar to polar rain at Earth—that is the electron flux can be assumed to be field-parallel. The flux median (Fig. 5, middle right) shows the electron precipitation in the quiet-time ionosphere close to the terminator. The precipitation is reduced above higher fields or regions of closed field lines. But in favorite conditions high maximum fluxes are observed down to the minimum altitude of observation (250 km) also for high crustal field strength. The higher maximum fluxes observed below 20 nT field strength are probable a statistical effect: Since high flux conditions are rare and more data samples measured above low fields the probability to encounter a high flux event is higher for these bins.

In the upper right region of the matrices in Fig. 5 we observe some bins with very high fluxes. These samples were taken during only 2 orbits which probably had high levels of precipitation of auroral type in the cusp structures above high-field regions.

5. Discussion and conclusions

We have used data of the ASPERA-3 ELS electron sensor on board the Mars Express spacecraft to investigate the intrusion of magnetosheath electrons into the martian atmosphere. Since the MEX spacecraft has no magnetometer on board it is not possible to do a strict separation into open and closed field regions as it has been done for the MGS MAG/ER dataset by Brain (2003). Nevertheless the excellent data coverage of MEX for altitudes between 250 and 1000 km allows us to determine

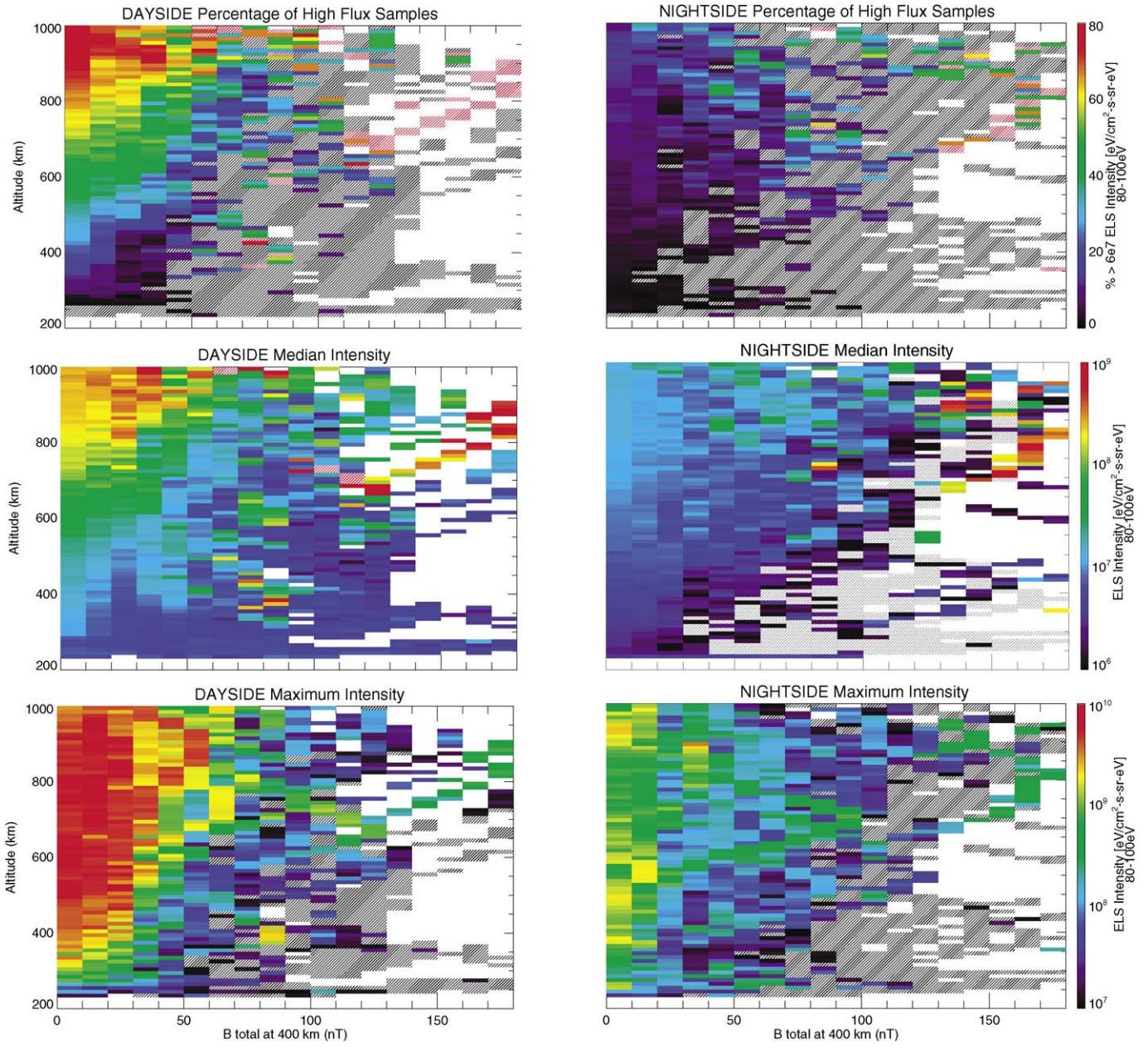

Fig. 5. Energy flux of 80–100 eV electrons measured by the electron sensor of the Mars Express ASPERA-3 instrument for all orbits between 1 Feb 2004 and 1 Mar 2005 as a function of total crustal field strength at 400 km altitude and MEX spacecraft altitude for dayside (left) and the nightside (right). The top panels show the percentage of samples above 6×10^7 eV/(cm^2 s sr eV), the middle panels median bin values and the bottom panels maximum bin values (see text for more details).

long time median and maximum electron fluxes as a function of the total crustal field strength at 400 km altitude using MGS field data from Connerney et al. (2001). We observe that in the magnetosheath electron energy fluxes are log-normally distributed with a median flux of 4×10^8 eV/(cm^2 s sr eV), on the dayside the flux distribution is bimodal with distinct log-normal populations centered around 10^7 eV/(cm^2 s sr eV) and 3×10^8 eV/(cm^2 s sr eV). We interpret this as the separation effect of the magnetic pile-up boundary (MPB). On the nightside we observe only the low flux population with a tail of rare events of higher flux. For both populations the crustal field have on average a shielding effect: above regions of low field the MPB can move closer to the planet and electrons inside of the MPB can precipitate to low altitudes.

To study the shielding efficiency of the crustal field the observed total field strength at 400 km altitude is sufficient to emphasize a significant correlation. To determine the average location of the MPB as a function of altitude and field strength we use the percentage of data samples above 6×10^7 eV/(cm^2 s sr eV) which is the energy flux where the sub-MPB and supra-MPB flux distributions are equal. It is surprising that using this simple proxy for the shielding we can observe a linear correlation between the average intrusion altitude (at the 50% level) and the total crustal field proxy on the dayside. Naturally the maximum fluxes do not show such a clear correlation since they depend on the radial extending local cusps and temporal effects. Here electron transport codes can be applied (Liemohn et al., 2003) and the observations can be com-

pared to particle simulations of mini-magnetospheres (Harnett and Winglee, 2003). We also tested to use just the horizontal component of the field since the shielding is most efficient perpendicular to the vertically intruding electrons (Verigin et al., 2004) but using the total field strength makes the linear dependence between field and intrusion altitude more visible. Instead of using the observed crustal field at 400 km altitude one could use an extrapolation of the field to other altitudes using the models by Cain et al. (2003) or Langlais et al. (2004). But at least on the dayside the solar wind pressure and interplanetary field will have a strong influence on the local field structure reducing the applicability of pressure-free extrapolations.

At the time of observation (1 Feb 2004 to 1 Mar 2005) the martian south pole was in winter (winter solstice was in October 2004). This means that the southern crustal fields did not reach solar zenith angles below 30°. The dayside shielding, we can observe in this dataset, is thus mainly due to the crustal field effects between −30° and −90°. Data from the MEX extended mission when the South pole will point towards the Sun may show a slightly different dependence.

The observations of the electron intrusion height have to be supplemented by a respective study of the proton intrusion using the ASPERA-3 IMA data. Single case studies showed already that solar wind protons can intrude to altitudes below 300 km (Lundin et al., 2004). The ion intrusion has direct influence on the oxygen ionization and the escape of ions and energetic neutral atoms from the martian atmosphere.

Acknowledgments

The ASPERA-3 experiment on the European Space Agency (ESA) Mars Express mission is a joint effort between 15 laboratories in 10 countries, all sponsored by their national agencies. We thank all these agencies as well as the various departments/institutes hosting these efforts. We wish to acknowledge support from DLR Grant 50QM99035 and Deutsche Forschungsgemeinschaft Grant WO 910/1-1. We also wish to acknowledge the Swedish National Space Board for their support of the main PI-institute and we are indebted to ESA for their courage in embarking on the Mars Express program, the first ESA mission to the red planet. We thank the members of the Mars Global Surveyor MAG/ER team for providing the Martian crustal field data.

References

Acuña, M., Connerney, J., Wasilewski, P., Lin, R., Anderson, K., Carlson, C., Mcfadden, J., Curtis, D., Mitchell, D., Rème, H., Mazelle, C., Sauvaud, J., d'Uston, C., Cros, A., Medale, J., Bauer, S., Cloutier, P., Mayhew, M., Winterhalter, D., Ness, N., 1998. Magnetic field and plasma observations at Mars: Initial results of the Mars Global Surveyor mission. Science 279 (5357), 1676–1680.

Acuña, M., Connerney, J., Wasilewski, P., Lin, R., Mitchell, D., Anderson, K., Carlson, C., Mcfadden, J., Reme, H., Mazelle, C., Vignes, D., Bauer, S., Cloutier, P., Ness, N., 2001. Magnetic field of Mars: Summary of results from the aerobraking and mapping orbits. J. Geophys. Res. 106 (E10), 23403–23417.

Barabash, S., Lundin, R., Andersson, H., Gimholt, J., Holmström, M., Norberg, O., Yamauchi, M., Asamura, K., Coates, A.J., Linder, D.R., Kataria, D.O., Curtis, C.C., Hsieh, K.C., Fedorov, B.R.S.A., Grigoriev, A., Budnik, E., Grande, M., Carter, M., Reading, D.H., Koskinen, H., Kallio, E., Riihela, P., Sles, T., Kozyra, J., Krupp, N., Livi, S., Woch, J., Luhmann, J., McKenna-Lawlor, S., Orsini, S., Cerulli-Irelli, R., Mura, A., Roelof, A.M.E., Williams, D., Sauvaud, J.-A., Winningham, J.-J.T.D., Frahm, R., Scherrer, J., Wurz, J.S.P., Bochsler, P., 2004. The Analyzer of Space Plasmas and Energetic Atoms (ASPERA-3) for the European Mars Express Mission. ESA publication SP-1240, pp. 121–139.

Bertaux, J.-L., Leblanc, F., Witasse, O., Quemerais, E., Lilensten, J., Stern, S., Saandel, B., Korablev, O., 2005. Discovery of an aurora on Mars. Nature 435, 790–794, doi:10.1038/nature03603.

Brain, D., 2003. The influence of crustal magnetic sources on the topology of the martian magnetic environment. Ph.D. thesis, Univ. of Colorado.

Brain, D., Bagenal, F., Acuña, M., Connerney, J., 2003. Martian magnetic morphology: Contributions from the solar wind and crust. J. Geophys. Res. 108 (A12), doi:10.1029/2002JA009482.

Cain, J.C., Ferguson, B.B., Mozzoni, D., 2003. An $n = 90$ internal potential function of the martian crustal magnetic field. J. Geophys. Res. 108 (E2), 1–19.

Connerney, J., Acuña, M., Wasilewski, P., Kletetschka, G., Ness, N., Rème, H., Lin, R., Mitchell, D., 2001. The global magnetic field of mars and implications for crustal evolution. Geophys. Res. Lett. 28 (21), 4015–4018.

Connerney, J., Acuña, M., Ness, N., Spohn, T., Schubert, G., 2004. Mars crustal magnetism. Space Sci. Rev. 111 (1–2), 1–32.

Crider, D., 2004. The influence of crustal magnetism on the solar wind interaction with Mars: Recent observations. Adv. Space Res. 33 (2), 152–160.

Crider, D., Acuña, M., Connerney, J., Vignes, D., Ness, N., Krymskii, A., Breus, T., Rème, H., Mazelle, C., Mitchell, D., Lin, R., Cloutier, P., Winterhalter, D., 2002. Observations of the latitude dependence of the location of the martian magnetic pileup boundary. Geophys. Res. Lett. 29 (8), 1170–1173.

Harnett, E.M., Winglee, R.M., 2003. The influence of a mini-magnetopause on the magnetic pileup boundary at Mars. Geophys. Res. Lett. 30, 1–10.

Langlais, B., Purucker, M.E., Mandea, M., 2004. Crustal magnetic field of Mars. J. Geophys. Res. 109 (E18), doi:10.1029/2003JE002048.

Liemohn, M.W., Mitchell, D.L., Nagy, A.F., Fox, J.L., Reimer, T.W., Ma, Y., 2003. Comparisons of electron fluxes measured in the crustal fields at Mars by the MGS magnetometer/electron reflectometer instrument with a B field-dependent transport code. J. Geophys. Res. 108 (E1), 1–16.

Lillis, R., Mitchell, D., Lin, R., Connerney, J., Acuña, M., 2004. Mapping crustal magnetic fields at Mars using electron reflectometry. Geophys. Res. Lett. 31 (15), doi:10.1029/2004GL020189.

Lundin, R., Barabash, S., Andersson, H., Holmström, M., Grigoriev, A., Yamauchi, M., Sauvaud, J., Fedorov, A., Budnik, E., Thocaven, J., Winningham, D., Frahm, R., Scherrer, J., Sharber, J., Asamura, K., Hayakawa, H., Coates, A., Linder, D., Curtis, C., Hsieh, K., Sandel, B., Grande, M., Carter, M., Reading, D., Koskinen, H., Kallio, E., Riihela, P., Schmidt, W., Säles, T., Kozyra, J., Krupp, N., Woch, J., Luhmann, J., Mckenna-Lawler, S., Ceruw-Irelli, R., Orsini, S., Maggi, M., Mura, A., Milillo, A., Roelof, E., Williams, D., Livi, S., Brandt, P., Wurz, P., Bochslers, P., 2004. Solar wind-induced atmospheric erosion at Mars: First results from ASPERA-3 on Mars Express. Science 305 (5692), 1933–1936.

Press, W., Teukolsky, S., Vetterling, W., Flannery, B., 1992. Numerical Recipes in C, second ed. Cambridge Univ. Press, Cambridge, UK.

Soobiah, Y., and 42 colleagues, 2006. Observations of magnetic anomaly signatures in Mars Express ASPERA-3 ELS data. Icarus 182, 396–405.

Verigin, M., Vignes, D., Crider, D., Slavin, J., Acuña, M., Kotova, G., Remizov, A., 2004. Martian obstacle and bow shock: Origins of boundaries anisotropy. Adv. Space Res. 33, 2222–2227.

Vignes, D., Acuña, M., Connerney, J., Crider, D., Rème, H., Mazelle, C., 2002. Factors controlling the location of the bow shock at Mars. Geophys. Res. Lett. 29 (9), doi:10.1029/2001GL014513.

Vignes, D., Mazelle, C., Rème, H., Acuña, M., Connerney, J., Lin, R., Mitchell, D., Cloutier, P., Crider, D., Ness, N., 2000. The solar wind interaction with Mars: Locations and shapes of the bow shock and the magnetic pile-up boundary from the observations of the MAG/ER experiment onboard Mars Global Surveyor. Geophys. Res. Lett. 27 (1), 49–52.